Communication

Sorafenib Analogue and Its Rearranged Compound: Design, Synthesis, Their In Vitro Anticancer Activity and Crystal Structure of the Rearranged Compound Dichloromethane Solvate

Qunying Yu *

Posted Date: 24 January 2024

doi: 10.20944/preprints202401.1715.v1

Keywords: Sorafenib analogue; crystal structure; rearranged compound; anticancer activity

Article

Sorafenib Analogue and Its Rearranged Compound: Design, Synthesis, Their In Vitro Anticancer Activity And Crystal Structure of the Rearranged Compound Dichloromethane Solvate

Qunying Yu

School of Pharmacy and Life Science, Jiujiang University, Jiujiang 332000, China; qunyingyu@qq.com

Abstract: Cancer is a devastating disease with female breast cancer becoming the leading cause of global cancer morbidity. Herein we report the design and synthesis of a sorafenib analog **1A** and its base-promoted arranged compound **1A2**. Their *in vitro* cytotoxicity and potencies in EFGR inhibition study revealed that compound **1A** displayed good antiproliferative activity in MDA-MB-231 (breast) cells with an IC_{50} value of 16.18±1.42 μM. Crystallization **1A2** afforded **1A2a** as a solvate with dichloromethane which was explicitly confirmed by the single crystal X-ray diffraction analysis.

Keywords: Sorafenib analogue; crystal structure; rearranged compound; anticancer activity

1. Introduction

Cancer is a devastating disease, ranking as a leading cause of premature death worldwide. According to the International Agency for Research on Cancer, 19.3 million new cancer cases were diagnosed and almost 10.0 million cancer deaths were occurred worldwide in 2020, with female breast cancer occupying 11.7% of all cancer cases as the leading cause of global cancer morbidity[1]. An estimated 34 million new cancers are projected to occur in 2070, doubling the number relative to 2020, highlighting the desire need for potent anticancer agents[2].

Sorafenib, an orally active anticancer drug marketed as Nexavar by the companies Bayer (Leverkusen, Germany) and Onyx Pharmaceuticals (San Francisco, California)[3], was approved for the standard treatment of advanced renal cell carcinoma and advanced HCC[4]. It exhibited activity against a wide spectrum of tumor types, including renal cell, hepatocellular, breast, and colorectal carcinomas in the preclinical setting. Mechanism of actions can be ascribed to its multiple known protein kinase targets[5]. It is likely to modulate two biological pathways that are implicated in cancer by binding to and shutting down key receptor tyrosine-kinase enzymes[3].

Design and synthesis sorafenib analogs can be an efficient way to discover potent cancer therapeutic agents. The epidermal growth factor receptor (EGFR) is a receptor tyrosine kinase, functions an important role in cell proliferation, survival, migration, adhesion, and differentiation, and is a precious target for cancer drug development. Curiously, many third-generation of EGFR tyrosine kinase inhibitors contain a 2-amino-pyrimidine scaffold (Figure 1)[6]. Inspired by these structural property, in this study, we design to keep the left wing of Sorafenib unchanged, and the central 4-phenoxy-pyridine was changed to 2-(pyrimidin-2-ylamino)pyridine, and identified a novel Sorafenib analogue **1A**, capitalizing upon the scaffold hopping strategy (Figure 2). Captivating, **1A** could be rearranged to **1A2** under an efficient base condition. Crystallization **1A2** from mixed solvent of methanol and dichloromethane identified **1A2a** as a dichloromethane solvate (Figure 3). Then, the new compounds of **1A** and **1A2** were biologically evaluated for their *in vitro* cytotoxicity and potencies in EFGR inhibition (Table 3).

 doi:10.20944/preprints202401.1715.v1

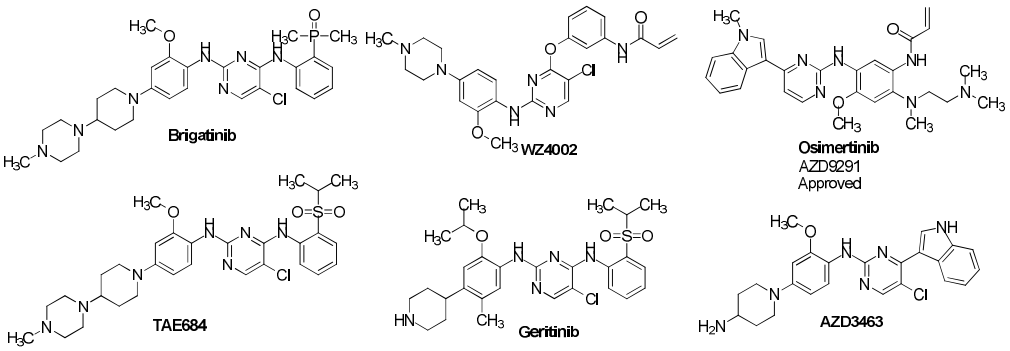

Figure 1. Third-generation of EGFR tyrosine kinase inhibitors with 2-amino-pyrimidine core.

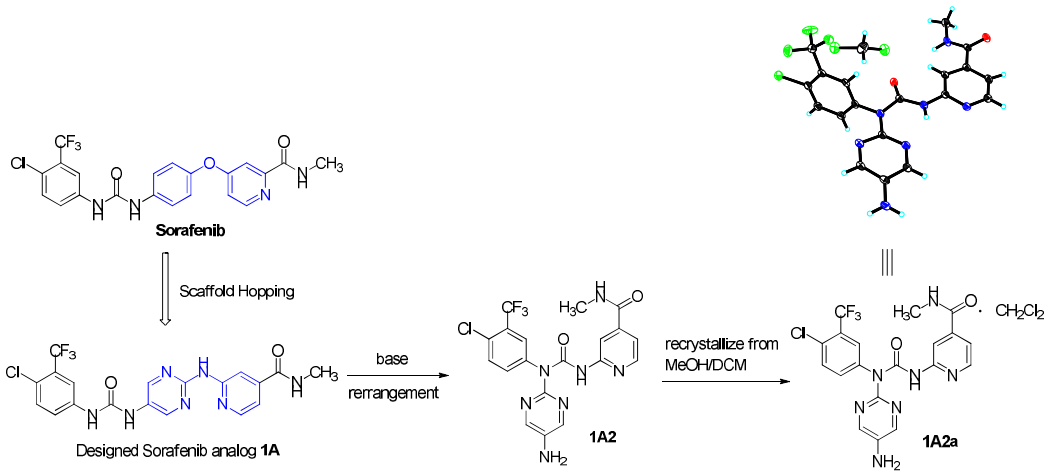

Figure 2. Design of Solafenib analogue utilizing a scaffold hopping strategy and its rearrangement product.

2. Results

2.1. Chemistry

A five-step sequence was developed to forge **1A** (Scheme 1). S_N2 reaction of methyl 2-aminopyridine-4-carboxylate with 2-chloro-5-nitropyrimidine, followed by nitro reduction (H_2, Raney Ni), afforded intermediate **3**, that underwent addition to 1-chloro-4-isocyanato-2-(trifluoromethyl)benzene, accomplishing the formation of intermediate **4**. Then hydrolysis of methyl ester of **4**, afforded carboxylic acid **5** that was transformed to carboxamide **1A** under coupling reagents condition (HATU, DIEA). Finally, base-mediated (NaH, DMF) rearrangement of **1A** delivered **1A2** (Figure 3) in high yield. Crystallization **1A2** from mixed solvent of methanol and dichloromethane obtained **1A2a** as a solvate with dichloromethane.

 doi:10.20944/preprints202401.1715.v1

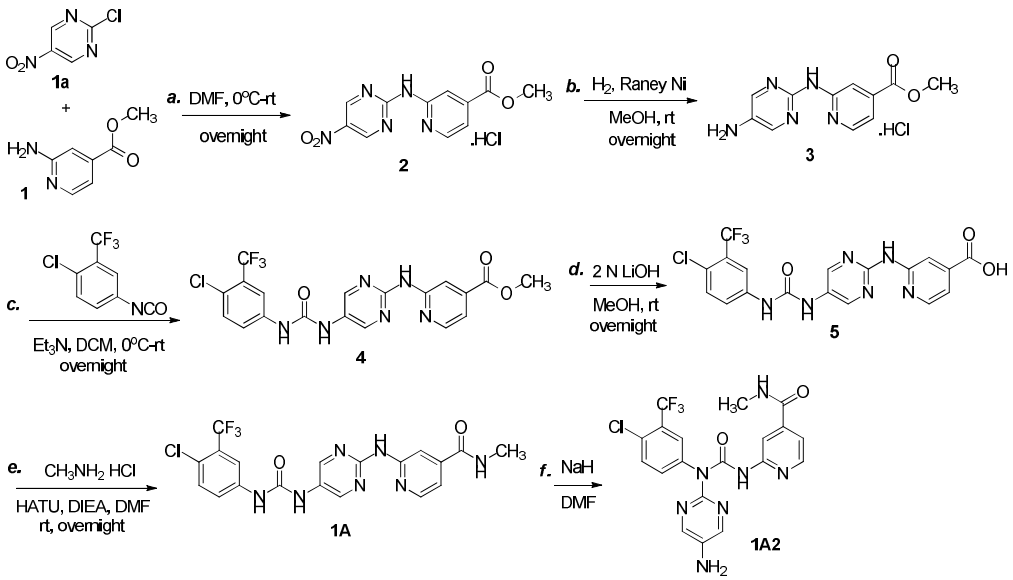

Scheme 1. Synthetic Route to the Molecule **1A** and **1A2**. Reagents and conditions: (a) **1a** (1.0 equiv), DMF, 0 °C, than added **1** (1.0 equiv), than rt (overnight); (b) H_2, Reny Ni, MeOH, rt, overnight; (c) **3** (1.0 equiv), Et_3N (2.0 equiv), DCM, 0 °C, than added **3a** (1.5 equiv), than rt (overnight); (d) **4** (1.0 equiv), MeOH, 2 N LiOH (2.0 equiv), rt (overnight); (e) **5** (1.0 equiv), DMF, HATU (1.5 equiv), Methylamine hydrochloride (4.0 equiv), DIEA (6.0 equiv), rt (overnight); (f) **1A** (1.0 equiv), DMF, 0 °C, NaH (3.0 equiv), than rt; DIEA = *N*,*N*-Ethyldiisopropylamine, HATU = 2-(7-Azabenzotriazol-1-yl)-N,N,N',N'-tetramethyluronium hexafluorophosphate.

2.2. Crystal structure of compound 1A2a

Single-crystal X-ray structure analysis reveals that compound **1A2a** is a dichloromethane solvate at the stoichiometric ratio 1:1 and crystallizes in the triclinic system space group *P*1 with lattice parameters of a = 0.98517(7) nm, b = 1.02973(7) nm and c = 1.14712(8) nm). The crystal size is 0.340×0.270×0.080 mm^3 (Table 1). The crystal structure analysis of interatomic distances in crystal **1A2a** indicates the presence of a set of intramolecular C-F7…H51-C, C-O10…H28-C, C-Cl1…C42-F, C-O10…C41 interaction, one N17…H12-N hydrogen bond and intermolecular C-O10…H48-C interaction formed between the carbonyl group and the solvate molecule (Table 2). By study and comparison their geometrical parameters, it is possible to suggest that all of these interactions are weak, except for N17…H12-N hydrogen bond (Figure 3). View of the pack drawing of **1A2a** is shown in Figure 4.

Table 1. Crystallographic Data of compound **1A2a.**

Formula	**$C_{19}H_{15}ClF_3N_7O_2 \cdot CH_2Cl_2$**	***F*(000)**	**560**
Formula weight	550.76	Crystal size / mm	0.340×0.270×0.080
Temperature / K	100(2)	θ range / (°)	3.90~72.42
Crystal system	Triclinic	Index ranges	-12<=h<=10, -12<=k<=12, -14<=l<=14
Space group	*P*1	Reflections collected, unique	18242
a / nm	0.98517(7)	R_{int}	0.0875
b / nm	1.02973(7)	Data, restraint, parameter	4496, 0, 317
c / nm	1.14712(8)	Goodness of fit on F^2	1.085
V / nm^3	1.14529(14)	Final R indices [$I>2\sigma(I)$]	R_1=0.0932, wR_2=0.2667

 doi:10.20944/preprints202401.1715.v1

Z	2	R_1 (all data)	0.1097,
D_c / (g•cm^{-3})	1.597	wR_2(all data)	0.2854
μ / mm^{-1}	4.164	$(\Delta\rho)_{max}$, $(\Delta\rho)_{min}$/ (e•nm^{-3})	773, -1183

Table 2. Selected bond, interatomic distances (nm) and torsion angles (°) for compound **1A2a.**

N16-C41	0.1444	N11-H12	0.0880	F8-C42	0.1339
N16-C29	0.1415	N11-C34	0.1391	F7-C42	0.1348
N16-C36	0.1409	N11-C36	0.1366	F6-C42	0.1313
C29-N33	0.1330	C34-N35	0.1346	N17-C43	0.1341
C13-N33	0.1338	C22-N35	0.1336	N17-C29	0.1335
F7-H51	0.2308	O10-H48	0.2215	Cl1-C42	0.3104
O10-C41	0.2604	O10-H28	0.2243	N33-C41	0.2641
H12-N17	0.1935	N11-N17	0.2647		

F6-C42-C52-C50	114.624	F8-C42-C52-C15	57.378	N16-C29-N33-C13	176.909
F7-C42-C52-C15	175.694	N16-C41-C50-C52	179.566	N30-C24-C43-N17	176.285
C36-N16-C41-C39	103.99	C36-N16-C29-N33	168.588	C29-N16-C36-O10	179.692
C29-N16-C41-C50	99.556	C41-N16-C29-N17	176.294	C29-N16-C36-N11	0.717
C45-C15-C52-C42	177	H12-N11-C34-N35	6.627	H12-N11-C36-O10	175.811

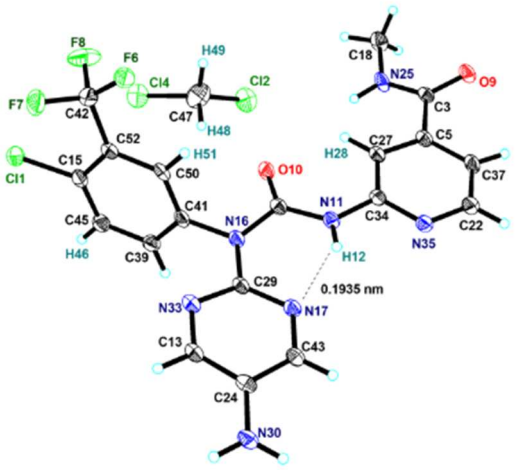

Figure 3. An ORTEP view the asymmetric unit of compound **1A2a** with displacement ellipsoids drawn at the 30% probability level and intramolecular hydrogen bond interaction.

 doi:10.20944/preprints202401.1715.v1

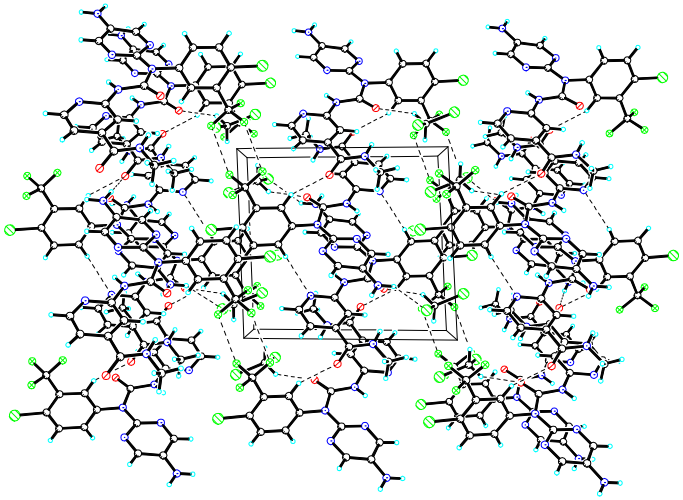

Figure 4. The pack drawing of compound **1A2a** with hydrogen-bonds shown as dashed lines.

2.3. Biology

The cytotoxicity of compound **1A**, **1A2** on five human cancer cell lines, including A549 (lung), HepG-2 (hepatocellular carcinoma, HCC), HCT116 (colon carcinoma), MDA-MB-231 (breast), PC-3 (prostate) were determined by an MTS method (Table 3). The effect of the two compounds on EGFR kinase was assessed using the EGFR Kinase Enzyme System (Promega) (Table 3). Cytotoxicity results showed that compound **1A** displayed good antiproliferative activity in MDA-MB-231 (breast) cells with an IC_{50} value of 16.18±1.42 μM. However, it was found to be ineffective on other cell lines. To our disappointment, compound **1A2** exerted no potencies in the five cancer cell lines (IC_{50}s＞40 μM). Both compounds show little ability to inhibit the EGFR kinase, with compound **1A2** displayed relatively higher inhibition percentage than compound **1A** at 40 μM concentration.

Table 3. Human Cancer Cell Growth Inhibition and percentage of EGFR kinase inhibition of compounds **1A** and **1A2.**

compd	$IC_{50}(\mu M)^a$					EGFR(%)[b]
	A549	HepG2	HCT116	MDA-MB-231	PC-3	
1A	>40	>40	>40	16.18±1.42	>40	13.55±0.50
1A2	>40	>40	>40	>40	>40	34.04±1.72

Note: Data from triplicate experiments were expressed as mean ± SD. [a] IC_{50} values represent the concentration needed to inhibit cancer cell line proliferation by 50%. [b]Percentage of kinase inhibition obtained at 40 μM of the test compounds.

3. Experimental Section

3.1. Materials and physical measurements

NMR spectra were recorded on Bruker DRX-400 instrument with TMS as internal standard. The Chemical shifts (δ ppm) are calibrated with reference to the deuterated solvent DMSO (δ 2.50 for ^{1}H NMR and 39.52 for ^{13}C NMR); CD_3OD (δ 3.31 for ^{1}H NMR and 49.00 for ^{13}C NMR), and coupling constants (*J*) are given in Hz. Silica gel column chromatography (200-300 mesh) was performed with various combinations of dichloromethane and methanol as eluent to purify compounds. ESI-MS analysis was determined on API QSTAR Pulsari spectrometer. Infrared spectra were recorded on a FT-IR spectrometer with KBr pellets. Yields refer to purified, dried and spectroscopically (^{1}H NMR) homogeneous material. All the commercial chemicals were used without further purification.

3.2. Crystal structural determination

The crystal data for compound **1A2a** was collected at 100(2) K on APEX DUO using Cu *Kα* radiation (*λ* = 1.54178Å). Data absorption corrections were applied using Semi-empirical from equivalents methods. This structure was solved using refinement method of full-matrix least-squares against F^2 with all non-hydrogen atoms anisotropic and hydrogen atoms isotropic. The final R_1 values were 0.0932 with $I > 2\sigma(I)$. Maximum and minimum transmission factors were 0.73 and 0.29, respectively. 18242 unique reflections were measured giving 4496 independent reflections (R_{int} = 0.0875). An ORTEP representation of the coordination environment of the compound **1A2a** including the atom labeling scheme is shown in Figure 3. The diffraction data is listed in Table 1. The selected bond, interatomic distances and torsion angles is listed in Table 2.

3.3. Cancer Cell Growth Inhibition Assay

The human tumor cell lines A549, HepG2, HCT116, MDA-MB-231, and PC-3 which were obtained from ATCC (Manassas, VA, USA) were cultured in Dulbecco's modified Eagle's medium (DMEM) or RMPI-1640 containing 10% heat-inactivated fetal bovine serum (FBS) at 37 °C in 5% CO_2, then seeded in 96-well plates at the concentration of 3000-5000 cells per well for 12-24 h when they were growing exponentially. The cells were treated with all compounds in different concentrations in triplicates, and incubated for another 48 h. A 20 *μ*L of 3-(4,5-dimethylthiazol-2-yl)-5-(3-carboxymethoxyphenyl)-2-(4-sulfopheny)-2H-tetrazolium, inner salt (MTS, 1.9 mg/mL) and 100 *μ*L culture medium were added to all wells and stained for 2-4 h at 37°C. The absorbance was measured with a MULTISKAN FC reader at *λ* = 492 nm. Data from triplicate experiments were expressed as mean ± SD. The IC_{50} value of each compound was calculated using Reed and Muench's method.

3.4. Cell-free EGFR Kinase Assay

The inhibitory percentage against EGFR kinase of compounds **1A, 1A2** at 40 *μ*M was measured using the EGFR Kinase Enzyme System (Promega). Operation steps strictly followed instructions from the manufacturer. EGFR (3 units/reaction), reaction buffer A, $MnCl_2$, DTT and peptide substrate were added to compound and incubated at 30 °C for 10 min followed by addition of ATP and an hour incubation at 30 °C. ADP-Glo™ Reagent was then added and incubated for another 40 min at 30 °C. A final 30 min incubation was needed after the addition of the Kinase Detection Reagent. Luminescence was measured using FlexStation 3.

3.5. Synthesis of Methyl 2-(N-(5-nitropyrimidin-2-yl)amino)pyridine-4-carboxylate hydrochloride (2)

To a solution of methyl 2-aminopyridine-4-carboxylate (**1)** (10.0 g, 65.8 mmol) in DMF (150 mL) was added 2-chloro-5-nitropyrimidine (10.5 g, 65.8 mmol) at 0 °C. Then mixture was warmed to room temperature and stirred overnight under nitrogen atmosphere. Upon completion of the reaction as indicated by TLC, the mixture was vacuum-filtered,and the filter cake was purified via silica gel column chromatography with DCM and MeOH as the eluent (10: 1 DCM: MeOH) to afford compound **2** as a yellow solid (13.0 g, 63%). ^{1}H NMR (400 MHz, DMSO-d_6) δ 11.17 (br s, 1 H), 10.12 (br s, 1 H), 9.85 (s, 2 H), 8.67 (d, *J* = 7.4 Hz, 1H), 8.04 (s, 1 H), 7.27 (d, *J* = 7.3 Hz, 1H), 3.95 (s, 3 H); IR (KBr) ν_{max} (cm^{-1}): 3430, 3234, 3033, 2958, 2852, 1732, 1671, 1606, 1531, 1418, 1349, 1277, 1116, 867, 765, 648, 532, 429; ESI-MS displays a peak at *m/z* 276.1, calcd for $[M + H]^+$: 276.2282.

3.6. Synthesis of Methyl-2-(N-(5-aminopyrimidin-2-yl)amino)pyridine-4-carboxylate hydrochloride (3)

To a solution of compound **2** (13.0 g, 41.7 mmol) in MeOH (100 mL) was added Raney Ni (3.0 g). The reaction mixture was degassed and back filled with hydrogen for three times, then attached to a hydrogen source, stirred vigorously at room temperature overnight. The catalyst was removed by filtration and the filtrate was concentrated to give a crude material which was purified by flash column chromatography (silica, 10: 1 DCM: MeOH) to yield compound **3** as a yellow solid (5.2 g, 44.2%). ^{1}H NMR (400 MHz, CD_3OD) δ 8.77 (d, *J* = 7.4 Hz, 1H), 8.31 (s, 2 H), 7.72 (d, *J* = 1.6 Hz, 1 H), 7.32 (dd, J_1 = 7.4 Hz, J_2 = 1.6 Hz, 1 H), 4.00 (s, 3 H); IR (KBr) ν_{max} (cm^{-1}): 3414, 3236, 3119, 1723, 1674, 1627, 1583, 1441, 1301, 1204, 996, 831, 756, 721, 669, 553; ESI-MS displays a peak at *m/z* 246.4, calcd for $[M + H]^+$: 246.2453.

3.7. Synthesis of 1-(4-chloro-3-(trifluoromethyl)phenyl)-3-(2-((4-(methyloxycarbonyl)pyridine-2-yl)amino)Pyrimidin-5-yl)urea (4)

To a solution of compound **3** (5.2 g, 18.4 mmol) and Et_3N (3.7 g, 36.8 mmol) in DCM (100 mL) was added 1-chloro-4-isocyanato-2-(trifluoromethyl)benzene (7.0 g, 31.8 mmol) at 0 °C. Then the reaction progressed at room temperature overnight. Upon completion the reaction, the mixture was washed with brine (30 mL x 3), dried over Na_2SO_4, and evaporated under vacuum to give a crude material, which was purified via silica gel column chromatography with DCM and MeOH as the eluent (10: 1 DCM: MeOH) to afford compound **4** as a yellow solid (5.0 g, 58%). ^{1}H NMR (400 MHz, CD_3OD) δ 9.34 (s, 1 H), 9.25-9.10 (m, 1 H), 8.38 (s, 2 H), 8.07 (s, 1 H), 7.84 (d, J = 6.7 Hz, 1 H), 7.75 (dd, J_1 = 8.7 Hz, J_2 = 2.3 Hz, 1 H), 7.58 (d, J = 8.8 Hz, 1 H), 4.06 (s, 3 H); IR (KBr) ν_{max} (cm^{-1}): 3387, 3344, 3214, 3120, 2928, 1735, 1679, 1583, 1556, 1435, 1334, 1200, 1131, 902, 836, 759, 722; ESI-MS displays a peak at m/z 467.3, calcd for $[M + H]^+$: 467.8090.

3.8. Synthesis of 1-(4-chloro-3-(trifluoromethyl)phenyl)-3-(2-(4-carboxypyridine-2-yl)amino)Pyrimidin-5-yl)urea (5)

To a solution of compound **4** (5.0 g, 10.7 mmol) in MeOH (100 mL) was added 2 N LiOH (10.7 mL, 21.4 mmol). The mixture was stirred at room temperature overnight. After consumption of the starting material, the mixture was acidified with 2 N HCl to pH 6-7, then concentrated to afford compound **5** as a yellow solid, which was used in the next step without further purification. LC-MS retention time 3.907 minute. ESI-MS displays a peak at m/z 453.0, calcd for $[M + H]^+$: 452.7745.

3.9. Synthesis of 1-(4-chloro-3-(trifluoromethyl)phenyl)-3-(2-((4-(methylaminocarbonyl)pyridine-2-yl)amino)Pyrimidin-5-yl)urea (1A)

A flask was charged with HATU (7.5 g, 19.7 mmol) and dissolved in DCM/DMF (1: 1) (60 mL), followed by immersion in an ice bath at 0 °C, then compound **5** (5.9 g, 13.0 mmol), methylamine hydrochloride (3.5 g, 51.8 mmol) and DIEA (10.1 g, 78.1 mmol) were added to the cold solution. The mixture was flushed with nitrogen, progressed at room temperature overnight. Upon completion the reaction, the mixture was concentrated in *vacuo*, diluted with AcOEt (300 mL), washed with Saturated Na_2CO_3 (30 mL x 2) and Saturated NaCl (50 mL x 3), respectively. The organic phase was dried over Na_2SO_4, concentrated. The crude material was purified by silica gel column chromatography (10: 1 DCM: MeOH) to afford compound **1A** as a yellow solid (2.0 g, 33.0%). ^{1}H NMR (400 MHz, DMSO-d_6) δ 12.47 (s, 1H), 8.75-8.59 (m, J = 4.6 Hz, 1H), 8.43 (d, J = 5.1 Hz, 1H), 8.34 (s, 1H), 8.07 (s, 2H), 7.85 (d, J = 2.4 Hz, 1H), 7.79 (d, J = 8.5 Hz, 1H), 7.62 (dd, J = 8.5, 2.4 Hz, 1H), 7.42 (dd, J = 5.2, 1.4 Hz, 1H), 5.51 (s, 2H), 2.77 (d, J = 4.5 Hz, 3H); ^{13}C NMR (101 MHz, DMSO) δ 165.13, 152.77, 151.99, 150.22, 148.57, 143.91, 142.11, 140.15, 139.13, 135.44, 132.17, 129.32 (q, J = 20.5), 128.91 (q, J = 7.4), 127.02 (q, J = 35.3), 124.02, 121.30, 116.44, 110.91, 26.29; IR (KBr) ν_{max} (cm^{-1}): 3440, 3310, 3219, 3124, 1635, 1563, 1506, 1428, 1410, 1314, 1283, 1229, 1131, 1030, 943, 897, 824, 704, 657; ESI-MS displays a peak at m/z 466.0, calcd for $[M + H]^+$: 466.8242.

3.10. Synthesis of 1-((5-amino)Pyrimidin-2-yl)-1-(4-chloro-3-(trifluoromethyl)phenyl)-3-((4-(methylaminocarbonyl)pyridine-2-yl)urea (1A2)

A frame-dried round-bottomed flask was charged compound **1A** (932 mg, 2.0 mmol, 1.0 equiv) and sodium hydride (NaH) (240 mg, 6.0 mmol, 3.0 equiv, 60% dispersion in mineral oil), cooled to 0 °C, then DMF (15 mL) was added via syringe all at once. The resulting suspension was allowed to warm to room temperature over 5 min. Upon completion of the reaction, as indicated by TLC, water (30 mL) was added to quench the reaction and extracted with DCM (3 x 30 mL). The combined organic phase was dried over anhydrous Na_2SO_4 filtered, evaporated. The crude material was purified by silica gel column chromatography (10: 1 DCM: MeOH) to afford compound **1A2** as a brown solid (755 mg, 81%). ^{1}H NMR (400 MHz, DMSO-d_6) δ 9.17 (s, 1H), 8.76 (d, J = 4.4 Hz, 1H), 8.27 (s, 2H), 8.20 (s, 2H), 7.93 (d, J = 6.6 Hz, 1H), 7.81 (br s, 1H), 7.50 (br s, 1H), 6.76 (d, J = 6.5 Hz, 1H), 5.99 (s, 2H), 2.78 (d, J = 4.4 Hz, 3H); ^{13}C NMR (101 MHz, DMSO-d_6) δ 164.60, 159.90, 158.45, 148.22, 143.96, 142.96, 142.77,

140.69, 138.67, 131.46, 126.31 (q, J = 120.6), 124.32, 122.67, 121.60, 121.26, 117.49, 116.62 (q, J = 23.7), 105.72, 26.35; ESI-MS displays a peak at m/z 466.0, calcd for $[M + H]^+$: 466.8242; IR (KBr) ν_{max} (cm^{-1}): 3433, 3350, 3226, 1680, 1663, 1561, 1482, 1439, 1307, 1235, 1133, 1038, 827, 741, 683, 663, 606, 584, 504.

3.11. Synthesis of 1-((5-amino)Pyrimidin-2-yl)-1-(4-chloro-3-(trifluoromethyl)phenyl)-3-((4-(methylaminocarbonyl)pyridine-2-yl)urea dichloromethane solvate (1A2a)

Crystallization **1A2** from mixed solvent of methanol and dichloromethane afforded **1A2a** as a dichloromethane solvate at the stoichiometric ratio 1:1 as a brown triclinic crystal. **Crystal data.** $C_{19}H_{15}ClF_3N_7O_2 \bullet CH_2Cl_2$ **1A2a**, M = 550.76, triclinic, space group $P1$, a = 9.8517(7) Å, b = 10.2973(7) Å, c = 11.4712(8) Å, α = 86.802(3)°, β = 81.486(3)°, γ = 84.921(3)°, V = 1145.29(14) $Å^3$, Z = 2, D_{calc} = 1.597 g/cm^3, μ(CuK$_\alpha$) = 4.164 mm^{-1}, T = 100.(2) K, F(000) = 560, crystal size = 0.340 x 0.270 x 0.080 mm^3, intensities of 18242 reflections (4496 independent, R_{int} = 0.0875).

4. Conclusions

In conclusion, a sorafenib analog **1A** with good antiproliferative activity in MDA-MB-231 (breast) cells was designed and synthesized. Base-mediated (NaH) arrangement of compound **1A** delivered compound **1A2** which was crystallized from MeOH/DCM affording compound **1A2a** as a dichloromethane solvate at the stoichiometric ratio 1:1. The structure of compound **1A2a** was corroborated by the single crystal X-ray diffraction study. Both compounds **1A** and **1A2** show little ability to inhibit the EGFR kinase, with compound **1A2** displayed relatively higher inhibition percentage than compound **1A**. Further biological activity and mechanisms investigation is ongoing in the laboratory to broaden their applications.

Supplementary Materials: The following supporting information can be downloaded at: www.mdpi.com/xxx/s1, Figure S2: General Information ; Figure S2: ^{1}H NMR spectrum (400 MHz) of compound 2 in DMSO-d_6; Figure S3: ^{1}H NMR spectrum (400 MHz) of compound **3/4** in CD_3OD; Figure S4: ^{1}H/^{13}C NMR spectrum (400 MHz) of compound **1A** in DMSO-d_6; Figure S5: ^{1}H NMR spectrum (400 MHz) of compound **1A2** in DMSO-d_6; Figure S6: IR spectrum of **2/3**; Figure S7: IR spectrum of **4/1A2**; Figure S8: IR/ ESI-MS spectrum of **1A**; Figure S9: ESI-MS spectrum of **1A2**.

Author Contributions: Qunying Yu designed and performed the research, analyzed the data and drafted the manuscript.

Funding: Please add: This work was financially supported by Jiujiang Programs for Science and Technology Development (S2021QNZZ037).

Institutional Review Board Statement: Not applicable.

Informed Consent Statement: Not applicable.

Data Availability Statement: Data are contained within the article and supplementary materials.

Conflicts of Interest: The author declare no conflicts of interest.

References

1. Sung, H.; Ferlay, J.; Siegel, R.L.; Laversanne, M.; Soerjomataram, I.; Jemal, A,; Bray, F. Global Cancer Statistics 2020: GLOBOCAN Estimates of Incidence and Mortality Worldwide for 36 Cancers in 185 Countries. *CA-Cancer J. Clin*. **2021,** *71*, 209-249.
2. Soerjomataram, I; Bray, F. Planning for tomorrow: global cancer incidence and the role of prevention 2020-2070. *Nat. Rev. Clin. Oncol*. **2021**, *18*, 663-672.
3. Scudellari, M. Drug development: Try and try again. *Nature*, **2014**, *516*, S4–S6.
4. Kudo, M. Systemic Therapy for Hepatocellular Carcinoma: Latest Advances, *Cancers*, **2018**, *10*, 412-427.
5. Wilhelm, S. M.; Adnane, L.; Newell, P.; Villanueva, A.; Llovet, J. M.; Lynch, M. *Mol.* Preclinical overview of sorafenib, a multikinase inhibitor that targets both Raf and VEGF and PDGF receptor tyrosine kinase signaling, *Cancer Ther*. **2008**, *7*, 3129-3140.
6. Chen, L.; Fu, W.; Zheng, L.; Liu, Z.; Liang, G. Recent Progress of Small-Molecule Epidermal Growth Factor Receptor (EGFR) Inhibitors against C797S Resistance in Non-Small-Cell Lung Cancer, *J. Med. Chem*. **2018**, *61*, 4290-4300.

 doi:10.20944/preprints202401.1715.v1